

Organic electro-optic modulator using transparent conducting oxides as electrodes

Guoyang Xu, Zhifu Liu, Jing Ma, Boyang Liu, Seng-Tiong Ho

Department of Electrical & Computer Engineering, Northwestern University, 2145 Sheridan Rd, Evanston, Illinois, 60208

g-xu@northwestern.edu; sth@ece.northwestern.edu

Lian Wang, Peiwang Zhu, Tobin J. Marks

Department of Chemistry and Material Science Research Center, Northwestern University, 2145 Sheridan Rd, Evanston, Illinois, 60208

Jingdong Luo, Alex. K.Y. Jen

Department of Materials Science and Engineering, Box 352120, University of Washington, Seattle, Washington, 98195

Abstract: A novel organic electro-optic (EO) modulator using transparent conducting oxides (ZnO and In₂O₃) as electrodes is demonstrated for the first time. The modulator employs the poled guest-host chromophore/polymer material AJL8/APC having $r_{33}=35\text{pm/V}$ and is able to achieve a low $V_{\pi}=2.8\text{ V}$ switching voltage for an 8mm-long device at a wavelength of $1.31\mu\text{m}$. This corresponds to a $V_{\pi}=1.1\text{ V}$ switching voltage for a 1cm-long device in a push-pull configuration. The push-pull $V_{\pi}L$ figure of merit normalized for the EO coefficient is thus $1.1\text{V-cm}/(35\text{ pm/V})$, which is 3-4x lower than that can be achieved with a conventional modulator structure. The bottom electrode is ZnO grown by Metal-Organic Vapor Deposition (MOCVD) and top electrode In₂O₃ deposited using ion-beam assisted deposition. The top electrode is directly deposited on the guest-host organic material. The design and fabrication considerations for the modulator are also discussed.

©2005 Optical Society of America

OCIS codes: (190.4710) Optical nonlinearities in organic materials; (250.2080) Electro-optic polymers; (250.7360) Waveguide modulators.

References and links

1. N. Dagli, "Wide-Bandwidth Lasers and Modulators for RF Photonics," *IEEE Trans. Microwave Theory Tech.* **47**, 1151-1171 (1999).
2. L. R. Dalton, W. H. Steier, B. H. Robinson, C. Zhang, A. Ren, S. Garner, A. Chen, T. Londergan, L. Irwin, B. Carlson, L. Fifield, G. Phelan, C. Kincaid, J. Amend and A. Jen, "From molecules to opto-chips: organic electro-optic materials," *J. Mater. Chem.* **9**, 1905-1920 (1999).
3. Y. Shi, C. Zhang, H. Zhang, J. H. Bechtel, L.R. Dalton, B. Robinson, W. H. Steier, "Low (sub-1-Volt) half voltage polymeric electro-optic modulators achieved by controlling Chromophore shape," *Science*, **288**, 119-122 (2000).
4. P. Zhu, H. Kang, M. E. van der Boom, Z. Liu, G. Xu, J. Ma, D. Zhou, S. Ho, and T. J. Marks, "Self-assembled materials and devices that process light," in *Optical Materials in Defence Systems Technology*, Anthony W. Vere, James G. Grote, eds., *Proc. SPIE* **5621**, 105-116 (2004).
5. J. Luo, S. Liu, M. Haller, J. Kang, T. Kim, S. Jang, B. Chen, N. Tucker, H. Li, H. Tang, L. Dalton, Y. Liao, B. H. Robinson, and A. K-Y. Jen, "Recent progress in developing highly efficient and thermally stable nonlinear optical polymers for electro-optics," in *Organic Photonic Materials and Devices VI*, J. G. Grote, T. Kaino, eds. *Proc. SPIE* **5351**, 36-43 (2004).

6. Z. Liu, S. T. Ho, S. S. Chang, and T. J. Marks, "Waveguide Electro-Optic Modulator Based on Organic Self-Assembled Superlattice (SAS)," 2002 Conference on Lasers and Electro-Optic, **73**, CtuK5, 196-197 (2002).
7. P. Zhu, van der Boom ME, H. Kang, G. Evmenenko, P. Dutta, T. Marks "Realization of expeditious layer-by-layer siloxane-based self-assembly as an efficient route to structurally regular acentric superlattices with large electro-optic responses," *Chem. Mater.* **14**, 4982-4989 (2002)
8. M. Oh, H. Zhang, C. Zhang, H. Erlig, Y. Chang, B. Tsap, D. Chang, A. Szep, W. Sterier, H. Fetterman, L. Dalton, "Recent advances in electrooptical polymer modulators incorporating highly nonlinear Chromophore," *IEEE J. Sel. Top. Quantum Electron.*, **7**, 826-835 (2001).
9. H. Lee, W. Hwang, M. Oh, H. Park, T. Zyung and J. Kim, "High performance electro-optic polymer waveguide device", *Appl. Phys. Lett.* **71**, 3779-3781 (1997).
10. P. Tang, D. J. Towner, A. L. Meier, and B. W. Wessels, "Low-voltage, polarization-insensitive, electro-optic modulator based on a polydomain barium titanate thin film," *Appl. Phys. Lett.* **85**, 4615-4617 (2004).
11. J. G. Grote, J. S. Zetts, R. L. Nelson, F. K. Hopkins, L. R. Dalton, C. Zhang, W. H. Sterier, "Effect of conductivity and dielectric constant on the modulation voltage for optoelectronic devices based on nonlinear optical polymers," *Opt. Eng.* **40**, 2464-2473 (2001).
12. J. P. Drummond, S.J. Clarson, J. S. Zetts, F. K. Hopkins and S. J. Caracci, "Enhanced electro-optic poling in guest systems using conductive polymer-based cladding layers," *Appl. Phys. Lett.* **74**, 368-370 (1999)
13. J. Ni, H. Yan, A. Wang, Y. Yang, C. L. Stern, A. W. Metz, S. Jin, L. Wang, T. J. Marks, J. R. Ireland, C. R. Kannewurf, "MOCVD-derived highly transparent, conductive zinc- and tin-doped indium oxide thin films: precursor synthesis, metastable phase film growth and characterization, and application as anodes in polymer light-emitting diodes," *J. Am. Chem. Soc.*, **127**, 5613-5624 (2005).
14. E. Martin, M. Yan, M. Lane, J. Ireland, C. Kannewurf, R. P. H. Chang, "Properties of multilayer transparent conducting oxide films," *Thin Solid Films*, **461**, 309-315 (2004).
15. G. Xu, J. Ma, S. T. Ho, T. J. Marks, "Low-voltage electro-optic modulator structure using transparent conducting oxide with high conductivity-loss ratio as electrode," *IEEE LEOS Avionics Fiber Optics and Photonics Conference*, ThC 4, Minneapolis, 22 September 2005.
16. G.L. Li, C. K. Sun, S. A. Pappert, W. X. Chen, and P.K.L. Yu, "Ultrahigh-speed traveling-wave electroabsorption modulator-design and analysis", *IEEE Trans. Microwave Theory Tech.* **47**, 1177-1183 (1999).

1. Introduction

Recently, there has been great interest in reducing the switching voltage of electro-optic (EO) modulators to <1V for RF photonics applications [1,2]. Low switching voltages improve link gain of RF signals. Many effort has been put into reducing EO modulator switching voltage by synthesizing higher EO coefficient materials and by implementing improved device structures [2-11]. New organic [4,5,8] and inorganic materials [10] with high EO coefficients have been developed as have organics with long-term orientational stability [5]. In regarding to device design, the push-pull Mach-Zehnder configuration has been introduced to reduce the modulator switching voltage while RF transmission lines have been designed to optimize the RF and optical lightwave velocity match at high speeds. Although conducting polymers represent one means to reduce the voltage drop in the cladding layers [11,12]. The effectiveness of this approach is limited by polymers conductivity having the requisite optical properties ($\sim 10^{-5}$ S/cm [11]), which is too low to benefit high frequency operation.

In this letter, we demonstrate for the first time a novel low-voltage EO modulator structure using transparent conducting oxide (TCO) materials [13,14] as electrodes. Compared with conventional metallic electrodes, TCO electrodes have the advantages of low optical loss and adjustable conductivity. In this new structure, the thin film nonlinear EO material is sandwiched directly between conductive TCO electrodes and there is no additional voltage drop from the top and bottom cladding, thus significantly increasing the electric modulation field applied on the nonlinear EO material. As a result, the modulator switching voltage can be reduced significantly. Below, we refer to this type of modulator as a TCO modulator.

The application of TCOs as electrodes in waveguide devices requires that the optical loss of the TCO-based structure to be low while maintain useful conductivity for practical device fabrication. We have simulated that high-speed (Gbit/s) operation of TCO modulator will also be possible by engineering appropriately TCO's conductivity σ versus optical loss α (σ/α) ratio[15]. In this paper, we will describe the benefits of using TCO electrodes in an EO

modulator and a side conduction structure to avoid TCO index mismatch and high optical loss followed by the fabrication and characterization of the TCO modulator.

2. Benefit of TCO electrode in EO modulator

Table 1. Layer structure of a conventional EO modulator ^a.

Layer	Material	Refractive index@1.3 μm	Thickness (μm)
Top electrode	Metal	-	0.1
Top cladding	NOA74	1.55	2.0
EO material	AJL8/APC	1.56	1.5
Bottom cladding	SiO ₂	1.48	2.5
Bottom electrode	Metal	-	0.01
Substrate	GaAs	3.4	-

^a NOA74 = a UV curable epoxy; AJL8 = an organic donor-acceptor Chromophore; APC = amorphous polycarbonate host polymer.

Conventional modulators utilize metals as electrodes. Typical structural parameters are summarized in Table 1. To avoid the metal-induced optical loss in the waveguide, the thickness of the top and bottom cladding layers must be sufficiently thick that the optical field has nearly completely decayed before touching the metal electrodes. For example, for the EO modulator structure shown in Table 1, the typical thicknesses of the top and bottom claddings must be greater than 2 μm and 2.5 μm , respectively, to reduce the metal loss and substrate coupling loss to less than 0.1dB/cm. The required thick cladding layers substantially increase the modulator switching voltage.

Table 2. Layer structure of a TCO EO modulator.

Layer	Material	Refractive index@1.3 μm	Thickness (μm)
Top cladding	NOA74	1.55	0.8
Top electrode	TCO(In ₂ O ₃)	2	0.02
EO material	AJL8/APC	1.59	1.5
Bottom electrode	TCO(ZnO)	1.9	0.05
Bottom cladding	SiO ₂	1.45	2.5
Substrate	GaAs	3.4	-

The voltage drop across the cladding layer can be eliminated by placing TCO electrodes directly against the EO material. The device layer characteristics are summarized in Table 2. For the TCO modulator, the distance between the electrodes is now given by the EO layer. Importantly, for the same applied voltage, the TCO modulator gives a 3-4 times greater electric field across the EO layer, resulting in 3-4 times lower switching voltage compared to the conventional modulator structure. The exact magnitude of the field enhancement for the TCO modulator vs. the conventional modulator will depend on the structure of the nature of the TCO materials comprising the top and bottom electrodes and the EO modulator structure.

3. Side conduction structure

Currently, TCO materials are widely used in display applications. The optical loss of the TCO layer is not of great concern due to its small thickness used in display applications. However, in TCO modulator applications, the optical loss of the TCO layer is one of the most important factors since the modulator length will be in centimeters level typically. Another potential

limitation of TCO materials is its refractive index mismatch with the organic waveguide. TCO materials usually have higher refractive indices (~ 2.0) compared to most organic materials (~ 1.5) in the wavelength 1.3-1.5 μm range. To avoid the large optical loss and the refractive index mismatch introduced by the TCO layer, a side conduction modulator structure is suggested shown in cross-section in Fig. 1. The TCO layer thickness must be sufficiently thin so that the refractive index mismatch can be avoided and optical loss in the TCO layers made small. In present TCO modulator, the thickness of the bottom TCO electrode is 50nm ZnO and top TCO electrode is 20nm In_2O_3 . The optical confinement for the top and bottom TCO electrode is 0.7% and 0.2% respectively. The bulk optical loss coefficients of the ZnO and In_2O_3 TCO electrodes used in the fabrication are about 20/cm and 1000/cm, respectively, measured using the usual waveguide cutback method and a Y-splitter dual-waveguide-arm technique with TCO film as waveguide cladding only along one of the arms to obtain the differential absorption loss due to the TCO material. The growth method of the TCO electrodes will be discussed in section of fabrication. So the total optical loss of TCO electrodes is about 2/cm. With development of low refractive index and less optical loss TCO materials, the TCO modulator structure may eventually use TCO as the entire cladding layer. In that case a top-down conduction structure would further reduce switching voltage.

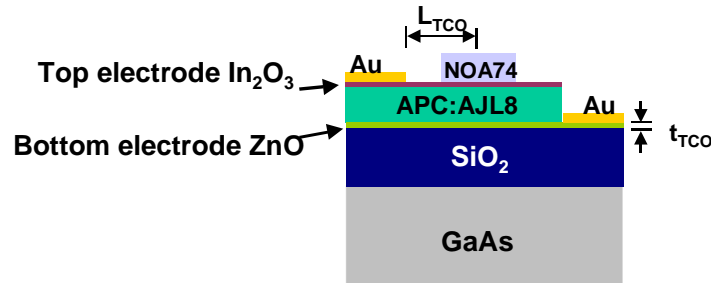


Fig. 1. Structure of a TCO modulator using poled AJL8/APC as the EO layer and ZnO and In_2O_3 as the electrodes.

4. High-speed performance simulation of the TCO modulator

The modulation bandwidth with different TCO conductivity for the structure in Fig. 1 was estimated using the traveling-wave model used in Ref. [16]. The TCO layers were modeled as a series resistance R_s to the modulator. The modulator is model as a capacitor with capacitance of C_m . The series resistance per unit length of the TCO layer can be expressed as: $R_s = L_{\text{TCO}}/(\sigma_{\text{TCO}} t_{\text{TCO}})$, where L_{TCO} is the distance between the waveguide and the metal transmission line, σ_{TCO} is the TCO material conductivity and t_{TCO} is the thickness of the TCO layer, as shown in Fig. 1.

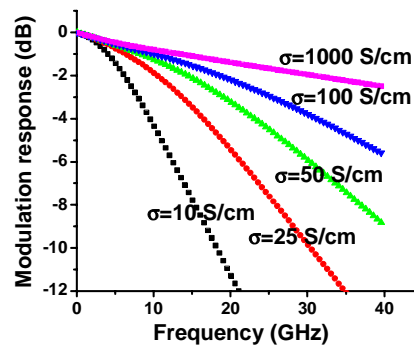


Fig. 2. Dependence modulation bandwidth on the conductivity of the TCO electrode.

In the simulation, the thickness of the TCO layers is assumed to be 50nm and $L_{\text{TCO}} = 5 \mu\text{m}$. The device length is assumed to be 8mm. Typical values of the metal transmission line conduction resistance $R_{\text{con}} = 3.5 \Omega\text{mm}^{-1}\text{GHz}^{-1/2}$ and the metal inductance $L_m = 0.1\text{-}1\text{ nH/mm}$ are used in the simulation [16]. Fig. 2 shows the dependence of the simulated modulation bandwidth versus the conductivity of the TCO electrode. It can be seen that with TCO conductivity $\sigma > 50 \text{ S/cm}$, the TCO modulator can operate above 20GHz. This magnitude of conductivity can be achieved using the TCO materials we developed as shown in section 3.

5. TCO modulator fabrication

Details of the TCO modulator fabrication are described in this section. A $2.8\mu\text{m}$ thick SiO_2 layer forming the bottom cladding was first deposited on a GaAs substrate wafer by PECVD. The refractive index of the SiO_2 layer was measured to be $n=1.45$ at the wavelength of $1.3 \mu\text{m}$. The required SiO_2 thickness was determined to keep the substrate coupling loss to less than 0.1dB/cm . Followed by the bottom TCO electrode: 50nm ZnO grown by low-pressure metal-organic chemical vapor deposition (MOCVD) at 450°C . The precursor for Zn was $\text{Zn}(\text{hfa})_2(\text{N,N}'\text{-DEEDA})$ which was purified by multiple vacuum-sublimation [13]. The conductivity, mobility, and carrier concentration of these ZnO films are measured to be 54.1 S/cm , $11.7 \text{ cm}^2/\text{Vs}$, $2.87 \times 10^{19}/\text{cm}^3$, respectively, by four-probe Hall effect measurements. The optical loss of these ZnO films are measured to be $\sim 20/\text{cm}$. The bottom ZnO electrode was patterned using standard photolithography and wet etching techniques. Nonlinear organic EO material AJL8/APC (25wt% AJL8 in amorphous poly(carbonate) (APC) host [5]) is then directly spin-coated on bottom ZnO electrode. The thickness of the EO layer is $\sim 1.5 \mu\text{m}$. A poling protective layer of $1.5\mu\text{m}$ poly-(4-vinylphenol) (PVP) is next spin-coated on before depositing the gold electrode for electrical field poling process. The film is then poled at 140°C with a poling voltage of 300 V for 5min, then cooled down to room temperature while maintaining the electrical field applied to the sample. After the poling process, the top metal electrode is etched away using conventional wet etching. The poling protective layer (the PVP layer) is then washed away with methanol. Subsequently, a 20nm In_2O_3 top electrode is deposited using an Ion-Beam Assisted Deposition (IAD) system. The top TCO electrode pattern is defined by a shadow mask. The In_2O_3 layer is deposited at room temperature at a pressure of 4mT with a deposition rate of 2.4nm/min . The carrier concentration is controlled via the O_2 partial pressure during deposition. The conductivity, mobility, and carrier concentration of the In_2O_3 film deposited are measured to be 70 S/cm , $30 \text{ cm}^2/\text{Vs}$, and $1.5 \times 10^{19}/\text{cm}^3$ respectively. The bulk optical loss of the IAD-deposited In_2O_3 is somewhat greater than that of the MOCVD deposited ZnO, $\sim 1000/\text{cm}$. Above the top electrode, a rib of spin-coated UV-cured NOA74 with thickness of $0.8 \mu\text{m}$ and width of $3\mu\text{m}$ is formed by O_2 RIE plasma etching. Photoresist is used as an etching mask.

6. Results and discussion

The switching voltage of the TCO modulator fabricated herein was measured using a single straight waveguide configuration. Light with $\lambda=1.31\mu\text{m}$ emitted from a DBF laser diode was coupled into the modulator waveguide using an optical lens. Two polarizers with polarization perpendicular to each other were used to analyze the phase change of the TE/TM mode after modulator. Details of the measurement setup can be found in Ref. [4]. The optical insertion loss of the 8mm-long modulator is 15dB ($\sim 9\text{dB}$ due to un-optimized coupling). Fig. 3 shows the typical EO response of the TCO modulator at a wavelength of $1.31\mu\text{m}$. Traces 1 and 2 represent the applied voltage signal and response signal of the modulator, respectively. The half-wave voltage V_π is measured to be 2.8V for a 8mm long waveguide. For electro-optical modulator, the relationship of switching voltage V_π and EO coefficient r is given by Eq. (1):

$$V_\pi = \frac{\lambda d}{n^3 r L \Gamma}. \quad (1)$$

where λ is the wavelength of the input light, d is the distance between the lower and the upper electrodes, n is the effective optical refractive index, L is the length of the electro-optic interaction region, and Γ is the optical mode overlap of the nonlinear material in the waveguide. The EO coefficient of the poled polymer is estimated to be ~ 35 pm/V using the above device parameters. Using the same poling conditions, the EO coefficient was measured to be 68 pm/V immediately after poling for controlled sample. The reduction in EO coefficient of the modulator sample is a result of the thermal exposure in post-poling process, e.g. metal deposition and photolithography. By optimization of the processing or using a higher T_g host material, we believe that this thermal relaxation can be reduced.

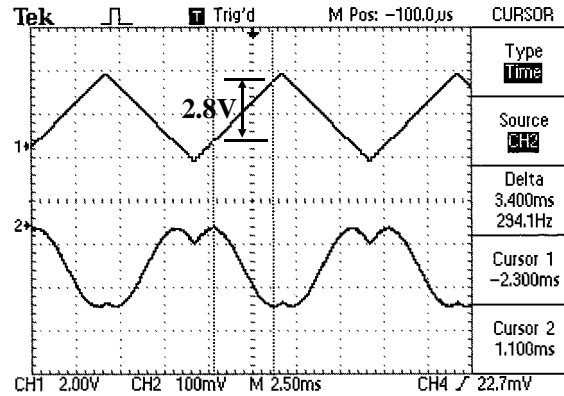


Fig. 3. Modulation response of the TCO modulator. Trace 1 is the applied voltage and trace 2 the optical intensity at the output side of the modulator.

For the conventional structure as shown in Table 1, using a polymer with the same EO coefficient, the switching voltage will be 3-4 times higher. The next step for TCO modulator development will be the demonstration of high-speed performance and characterizing the dependence of the modulation performance on the properties of the TCO materials.

7. Conclusions

We have realized a low-voltage organic electro-optical modulator for the first time using transparent conducting oxide (TCO) as electrodes. With this new structure, the switching voltage can be reduced by 3-4 times compared to a conventional modulator structure with the same EO-active material. Our initial modeling indicates that an optimized TCO modulator could potentially achieve a modulation frequency of 10-20GHz. The TCO modulator fabricated has a switching voltage of 2.8V (linear geometry) for an organic EO material with EO coefficient $r = 35$ pm/V and a device electrode length of only 8mm. These results show that a modulator with switching voltage of < 0.5 V should be achievable in a push-pull Mach-Zehnder configuration with a typical 2cm long device using TCO electrodes and optimized poling conditions.

Acknowledgments

This work is supported by the DARPA MORPH program under contract DARPA/ONR N00014-04-1-0093 and by the NSF MRSEC program under grant (DMR-0076097).